

Downstreaming of natural materials Huta Ginjang Quartz Sand doped with Nd₂O₃ for laser medium application

Juniastel RAJAGUKGUK^{1,*}, Juniar HUTAHEAN¹, C.S. SARUMAHA^{2,3}, Ricky A. SYAHPUTRA⁴, N. INTACHAI⁵, S. KOTHAN⁵, and J. KAEWKHAO^{3,6,*}

- ¹ Department of Physics, Faculty of Mathematics and Natural Sciences, Universitas Negeri Medan, Medan 20221, Indonesia
- ² Faculty of Science and Technology, Muban Chombueng Rajabhat University, Ratchaburi 70150, Thailand
- ³ Center of Excellence in Glass Technology and Materials Science (CEGM), Nakhon Pathom Rajabhat University, Nakhon Pathom 73000, Thailand
- ⁴ Department of Chemistry, Faculty of Mathematics and Natural Sciences, Universitas Negeri Medan, Medan 20221, Indonesia
- ⁵ Center of Radiation Research and Medical Imaging, Department of Radiologic Technology, Faculty of Associated Medical Sciences, Chiang Mai University, Chiang Mai 50200, Thailand
- ⁶ Physics Program, Faculty of Science and Technology, Nakhon Pathom Rajabhat University, Nakhon Pathom 73000, Thailand
- *Corresponding author e-mail: juniastel@unimed.ac.id, jakrapong@webmail.npru.ac.th

Received date:

30 January 2025

Revised date:

4 July 2025

Accepted date:

13 August 2025

Keywords:

Quartz sand; Neodymium (Nd3+); Laser Medium; Glasses

Abstract

The QSBoBa glasses with chemical formula 10 Quartz sand + (50-x) B₂O₃ + 10BaO + 30Na₂O + xNd₂O₃ (x = 0, 0.5, 1, 1.5, and 2 mol%) were prepared by a conventional melt-quenching technique. The successfully fabricated glass samples will be analyzed based on their physical, structural, optical and luminescent properties. The XRD and FTIR spectra have been included to observe the complete structural properties. Optical absorption spectra revealed several characteristic transitions, with a prominent hypersensitive transition ${}^{4}I_{9/2} \rightarrow {}^{4}G_{5/2}$ at 584 nm, indicating an increasing asymmetry and disorder at higher Nd³⁺ concentrations. The photoluminescence emission spectra demonstrated strong radiative transitions of ${}^4F_{3/2} \rightarrow {}^4I_{11/2}$, particularly the 1060 nm, which is critical for solid-state laser applications. The emission intensity decreased when the concentration of Nd3+ was increased. Decay lifetime analysis confirmed this trend, with longer lifetimes at 0.5 mol% and 1.0 mol% and shorter lifetimes at higher concentrations, suggesting quenching effects at elevated doping levels. Radiative parameters, including transition probability (A_R) and emission cross-section (σ_e), identified 0.5 mol% as the optimal doping concentration, achieving high radiative efficiency without significant quenching. The broad emission bandwidth at 1330 nm further indicates the material's potential for broadband optical amplifiers in telecommunications. The Nd3+-doped QSBoBa glass system exhibits promising properties for solid-state lasers, optical amplifiers and sensors, with 0.5 mol% offering the best balance between emission efficiency and structural stability. This study confirms the versatility and potential of the QSBoBa glass system for advanced photonic applications.

1. Introduction

The demand for efficient and high-performance laser materials has been a significant focus in modern optical research, driven by the widespread use of lasers in various industries, such as telecommunications, medicine and defense [1-3]. Rare-earth doped glasses, especially those containing neodymium ions (Nd³⁺), had attracted considerable interest due to their favorable optical and luminescence properties [4]. Neodymium-doped glasses were widely used in solid-state lasers because of their strong absorption in the near-infrared (NIR) region and efficient radiative transitions, making them ideal for applications like laser amplifiers, fiber lasers, and other photonic devices [5-7]. In recent years, attention has shifted toward the exploration of new host materials and the incorporation of sustainable, naturally sourced components for these glass systems [8-9]. The Nd³⁺ ion plays a critical role in laser media due to its ability to exhibit strong luminescence and radiative transitions, especially in the near-infrared region [10]. Boric oxide (B₂O₃) is commonly used as a glass former due to its low melting temperature and good chemical durability [11,12]. In addition to its role in glass formation, B₂O₃ contributes to the glass's optical properties by reducing the phonon energy of the matrix. This is particularly important for rare-earth doped glasses, as lower phonon energy reduces non-radiative relaxation processes, enhancing the radiative efficiency of the dopant ions [13,14]. BaO (Barium Oxide) enhances the glass's mechanical properties and improves its refractive index, contributing to the structural rigidity of the material [15]. Na₂O (Sodium Oxide) acts as a flux, lowering the melting point and aiding in glass formation [10].

The combination of several glass network formers, especially between borates and silicates, is currently the focus of attention in the development of optical materials. Silicates themselves continue to be developed by utilizing natural resources as raw materials, such as rice husk ash (RHA), sugarcane/ bagasse and quartz sand. Based on several studies, the silica content (SiO₂) in RHA ranges from 85% to 98% [16-20], while in sugarcane/bagasse it is around 63% to 68% [20,21]. Meanwhile, quartz sand (QS) is known to have a very high silica content, generally above 95% [22,23], making it a potential source of natural silica. In this study, quartz sand from Indonesia was chosen as the main raw material because of its abundant availability and high natural silica content. Quartz sand acts as a source of silica that not only increases the thermal and mechanical resistance of the material, but also supports its optical transparency [22]. Several previous studies have shown that quartz sand can be used in various photonic applications, including in the development of materials for deep-ultraviolet light-emitting diodes [24], scintillating application [22], bio-soluble silicate fibers [25] and laser application [26]. Therefore, this study will utilize quartz sand as the basis for the silicateborate glass system for optical applications, especially in the laser field.

Neodymium Oxide (Nd₂O₃) is the key dopant in this study, providing the rare-earth Nd³⁺ ions that are responsible for the glass's luminescence and radiative properties. Nd³⁺ ions have been extensively studied for their ability to emit light in the NIR region, particularly at wavelengths around 1060 nm, which is crucial for solid-state lasers [27]. The $^4F^{3/2} \rightarrow ^4I_{11/2}$ transition of Nd³⁺ ions is the primary emission pathway utilized in Nd-doped lasers, making Nd₂O₃ a valuable addition to the glass matrix [28]. The concentration of Nd₂O₃ in this study is varied from 0 mol% to 2 mol% to examine how different doping levels affect the glass's optical and luminescent properties. Higher concentrations of Nd₂O₃ are expected to enhance the luminescence intensity, but excessive doping can lead to concentration quenching, where energy transfer between adjacent Nd³⁺ ions reduced the overall emission efficiency. Therefore, finding the optimal doping level is critical for maximizing the performance of Nd-doped glasses in laser applications.

This study presents a novel approach to developing laser media by incorporating Huta Ginjang quartz sand as a natural source of silica in a Nd_2O_3 -doped borate glass system. The unique combination of naturally sourced quartz sand with the well-established advantages of Nd^{3+} -doped glasses offers a sustainable and cost-effective alternative to synthetic materials. By varying the Nd_2O_3 concentration, this research aims to systematically investigate the effects of Nd^{3+} doping on the physical, optical and luminescent properties of the glass samples. This research contributes to the growing field of sustainable materials for photonic applications and provides new insights into the use of natural materials in high-performance optical devices. The results of this study have the potential to impact not only laser technology but also other areas of photonics, such as fiber optics and optical amplifiers.

2. Experimental

The glass with the composition of 10 Quartz sand + (50-x) B₂O₃ + $10BaO + 30Na_2O + xNd_2O_3$ (x = 0, 0.5, 1, 1.5, and 2 mol%) underwent the fibrillation stage using melt-quenching. All prepared samples were labeled QSBoBa, QS(0.5)BoBaNd, QS(1.0)BoBaNd, QS(1.5)BoBaNd, and QS(2.0)BoBaNd, respectively. QS used in this study was collected from Huta Ginjang village, located in North Sumatra. To ensure the removal of impurities, the sand was thoroughly washed with water and

detergent for 24 h, then dried under direct sunlight for two days. After complete drying, the sand was mechanically milled using a ball mill for four hours to achieve a fine and homogeneous powder. The chemical composition of the QS was determined using X-ray fluorescence (XRF) analysis. The same QS processing method was adopted as outlined in our previous works [22,26]. All chemicals used in this study were of high analytical grade, with a purity of 99.9%. The QS itself exhibited a high SiO₂ content of 99.08%, with minor impurities including K₂O, CaO, Cr₂O₃ and Fe₂O₃, each contributing to less than 0.92% collectively. All components were accurately measured using a chemical balance before being placed into the alumina crucibles. Then, the glass composition mixture powders are melted in a furnace and continuous heat treatment is carried out to a temperature of 1100°C. After holding for 3 h at that temperature, samples will be shaped in the graphite mold before continuing to the annealing steps. The annealing process was carried out to reduce the thermal stress in the glass materials. This process was using a temperature of 500°C for 3 h. Furthermore, the glasses were removed from the annealing process after cooling to room temperature. The solidified glass samples were cut into small rectangular with size $1.0 \text{ mm} \times 1.5 \text{ mm} \times 0.3 \text{ mm}$ and polished to achieve optically smooth surfaces, ensuring that they were suitable for spectral measurements. The density of glass was determined using the Archimedes' principle by weighing a sample in both air and water using a very precise microbalance (AND, HR 200) with a 4-digit sensitivity. The refractive index was determined by using an Abbe refractometer (Atago, DR-M2 model) operating at a wavelength of sodium D-line ($\lambda = 589$ nm). X-ray Diffraction Shimadzu (XRD-6100) was used to examine crystalline structure (or lack thereof) of the glasses sample. The FTIR spectroscopy was measured using Agilent technologies Cary 630 FTIR spectrometer in the range 650 cm⁻¹ to 2000 cm⁻¹. FTIR was used to study the structural properties by analyzing the vibrational modes of the glass matrix, providing information on the functional groups present. Moreover, the optical absorption spectra of the samples were investigated by using of the UV-3600 Shimadzu Spectrophotometer. Absorption spectra were collected with a spectral resolution (step size) of 1 nm in the wavelength range of 350 nm to 1000 nm. Whereas, the luminescence spectra were employed to analyze the emission properties of the glass, particularly focusing on the radiative transitions of Nd3+ ions. Near-Infrared (NIR) luminescence spectra and decay time were recorded using the (QM)-300 spectrofluorometer manufactured by PTI-Horiba using laser diode source (808 nm).

3. Results and discussion

3.1 Samples view

The shape of the glass becomes one of the important things because the glass that has a high level of transparency, homogeneous, no cracks will be selected for the cutting and smoothing process. Figure 1 shows the appearance of a glass sample that was cut and polished to the optimum size before structural and optical characterization. As the concentration of Nd_2O_3 increased, the glasses progressively became more opaque and their color shifts from colorless (undoped) to a more pronounced purple hue. The addition of neodymium ions (Nd^{3+}) introduced absorption bands in the visible spectrum, causing the observed color changes. This progression is typical of glasses doped

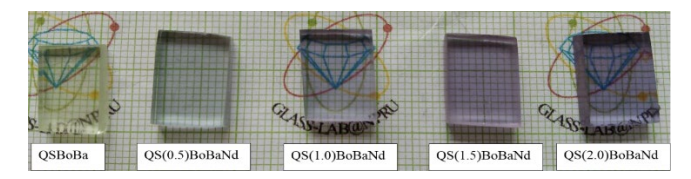


Figure 1. The physical shape of the quartz sand BoBa glasses doped with Nd³⁺ ion.

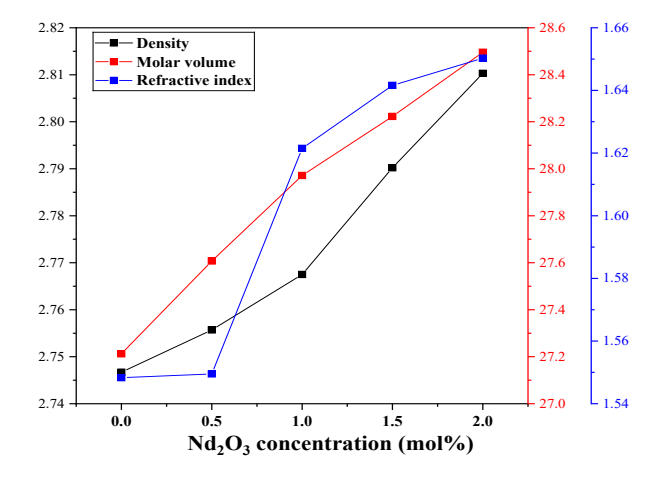


Figure 2. The relationship of density, molar volum and refractifity index of Nd³⁺ doped QSBoBa for five variations concentration.

with rare-earth elements like Nd, where increased doping results in higher light absorption, often leading to characteristic color changes due to the electronic transitions of Nd³⁺ ions [29].

3.2 Physical properties

Table 1 shows a set of physical properties for five glass samples based on quartz sand and borate glass doped with varying concentrations of Nd³⁺ from 0 mol% (undoped) to 2.0 mol%. The increasing concentrations of Neodymium oxide (Nd₂O₃) were followed with changes in some physical properties included with molar volume, density, refractive index and others parameters. As shown in Table 1, the density increases from 2.7467 g·cm⁻³ (undoped) to 2.8103 g·cm⁻³ (2.0 mol% doped) when the Nd³⁺ concentration is increased. It can be

attributed to the higher atomic mass of neodymium compared to the base constituents (B_2O_3 and QS), which results in a denser glass structure as more Nd_2O_3 is added [30,31].

The significant changes in the density, molar volume and refractive index parameters due to Nd3+ ions increases occurred as shown in Figure 2. The density of the glass increases consistently with increasing Nd₂O₃ concentration due to that Nd₂O₃ has a higher molecular weight than the base glass components (B₂O₃ and SiO₂), leading to a denser material as more Neodymium ions (Nd3+) are incorporated. The increased density had also suggested that the glass network had become more compact or denser with the incorporation of Nd3+ ions, which replaced lighter ions in the base glass structure. The increase in molar volume indicated that as Nd₂O₃ is added, the glass network expanded slightly due to the larger ionic radius of Nd³⁺ compared to the ions it replaced [32]. The rate of increase of molar volume starts to level off slightly after 1.5 mol% doping, suggested that the glass network may begin to reach a saturation point where additional Nd³⁺ ions do not significantly expand the structure further. The refractive index increases more steeply compared to the other properties, especially after 1.0 mol% Nd₂O₃. This shows that even small amounts of Nd3+ ions have a substantial effect on the optical properties of the glass. The increase in refractive index suggests that the glass becomes more optically dense with increased Nd₂O₃ concentration, making it more effective at bending light, which is consistent with the behavior of glasses doped with rare-earth elements like neodymium [33].

3.3 Structural properties

Figure 3 shows the X-ray diffraction (XRD) patterns of quartz sand-borate glass (QSBoBa) doped with varying concentrations of Nd₂O₃ (Neodymium Oxide). The XRD patterns are presented for five glass samples: undoped and doped with 0.5 mol%, 1.0 mol%, 1.5 mol%, and 2.0 mol% Nd₂O₃. The primary focus of this analysis is to identify the structural properties of these glasses based on the XRD spectra, which provide insight into the glass's crystallinity or amorphous nature. All the XRD spectra show broad, featureless humps rather than sharp, well-defined peaks. This indicates that all the glass samples, including those doped with Nd₂O₃, remain in an amorphous state. In amorphous materials, atoms or molecules are arranged in a disordered manner,

Table 1. The physical properties of Nd3+ doped QSBoBa medium glasses.

Measurement	Glass samples							
	QSBoBa	QS(0.5)BoBaNd	QS(1.0)BoBaNd	QS(1.5)BoBaNd	QS(2.0)BoBaNd			
Molar weight (g·mol ⁻¹)	74.7436	76.0779	77.4122	78.7465	80.0808			
Density (g·cm ⁻³)	2.7467	2.7557	2.7675	2.7902	2.8103			
Molar volume (cm ³ ·mol ⁻¹)	27.2123	27.6074	27.9714	28.2225	28.4957			
Ion concentration, N × 10 ²⁰ (ion·cm ⁻³)	-	1.0907	2.1529	3.2007	4.2267			
Polaron radius ×10 ⁻⁸	-	8.4333	6.7228	5.8904	5.3690			
Inter nuclear distance ×10 ⁻⁷	-	2.0930	1.6685	1.4619	1.3325			
Field strength, $F \times 10^{16}$ cm ²	-	0.8296	1.3054	1.7004	2.0467			
Refractive index (n)	1.5483	1.5495	1.6215	1.6416	1.6503			
Molar refractivity (Rm)	8.6467	8.7883	9.8447	10.1884	10.3973			
Molar electronic Polarization ×10 ⁻²⁴	3.4295	3.4856	3.9046	4.0410	4.1238			
Metallization Criteria (M)	0.6822	0.6817	0.6481	0.6390	0.6351			
Reflection loss (R) %	4.6295	4.6454	5.6206	5.8992	6.0206			
Dielectric constant (ε)	2.3972	2.4010	2.6293	2.6949	2.7235			
Thickness (cm)	0.30	0.30	0.30	0.30	0.30			

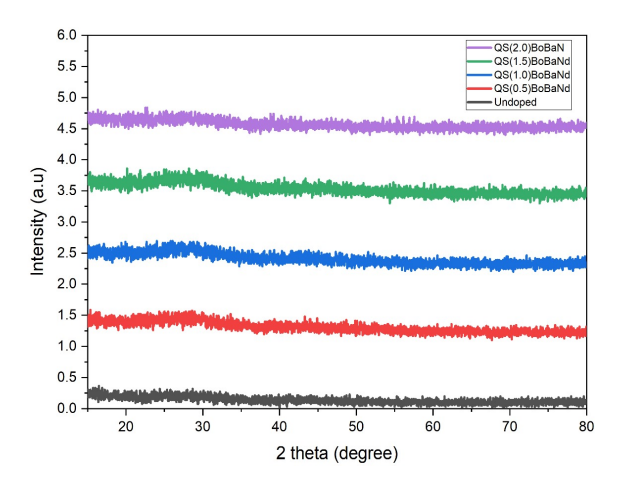


Figure 3. The XRD spectrum of Nd³⁺ doped QSBoBa glasses for five variations concentration.

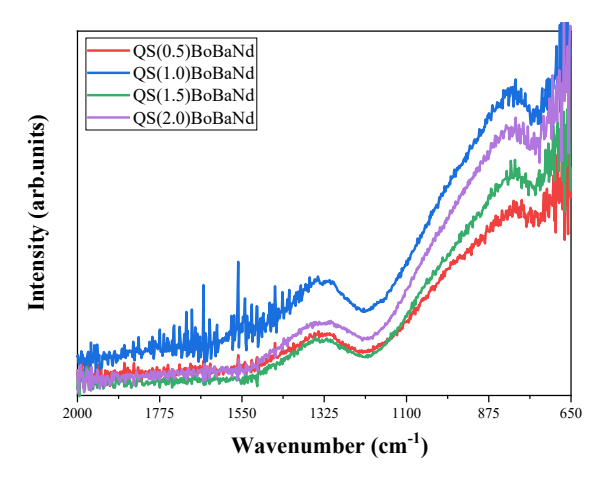


Figure 4. The FTIR spectrum of Nd³⁺ doped quartz sand-borate glass system with Nd³⁺ ion concentration of 0; 0.5; 1.0; 1.5; and 2.0 mol%.

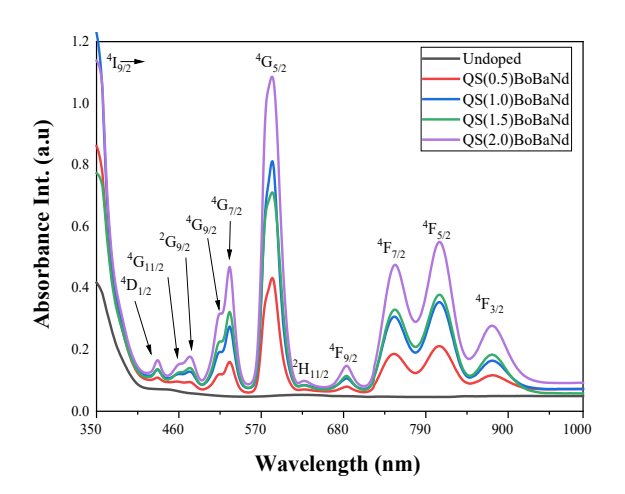


Figure 5. The Absorption spectra of Nd³⁺ doped quartz sand-Borate glass system with Nd³⁺ ion concentration of 0; 0.5; 1.0; 1.5; and 2.0 mol%

and broad peaks are typically observed in the XRD spectra instead of sharp Bragg peaks associated with crystalline materials. This is consistent with the typical XRD pattern of glasses, which are structurally disordered materials lacking long-range periodicity. This observation aligns with findings from various studies on borate glasses, such as those by Biradar, Shrikant et al. [34], who report broad halos in XRD patterns of rare-earth doped borate glasses, confirming the amorphous nature of the glass matrix. The broad hump in the XRD pattern usually arises from the short-range order of atoms in the glass network, which is characteristic of glassy materials. The XRD patterns suggest that Nd³⁺ ions did not cause the formation of new crystalline phases in the QS-borate glass network. This finding is consistent with other studies on rare-earth doped glasses, such as Sidebottom et al. [35] and Abo-Mosallam et al. [36], who have shown that even at higher concentrations, rare-earth elements like Nd3+ typically do not lead to crystallization within the glass matrix unless the doping concentration is exceedingly high or special heat treatments are applied. Instead, the rare-earth ions had tended to occupy interstitial sites within the glass network, acted as network modifiers and had not significantly disrupted the amorphous nature of the glass. The Fourier Transform Infrared (FTIR) spectra of quartz sand-borate glass (QSBoBa) doped with increasing concentrations of Nd3+ ions were shown in Figure 4. The FTIR spectroscopy provides insights into the vibrational modes of chemical bonds present in the glass network and how they evolve with the introduction of Neodymium Oxide. The general infrared absorption bands for QSBoBa glasses can be assigned as Table 2.

From the FTIR spectra of Nd³+-doped QSBoBa glass, it can be confirmed that the structural modifications induced by increasing concentrations of Neodymium oxide (Nd₂O₃). With higher Nd₂O₃ concentrations, it was observed that the structural disorder was increased as indicated by the disruption of B–O–B linkages and the formation of non-bridging oxygen atoms [37]. There has also been a transformation shifted of some trigonal BO₃ units into tetrahedral BO₄ units [38]. As Nd₂O₃ was introduced, the Nd³+ ions had acted as network modifiers, broken some of the existing borate chains and created non-bridging oxygen atoms. This was reflected in the decreased transmittance with increased Nd³+ concentrations, indicating increased structural disorder [33]. The presence of Nd³+ ions had also enhanced the formation of BO₄ tetrahedral units, which could absorb more in the infrared region.

3.4 Absorption spectra

Figure 5 illustrates the absorption spectra of quartz sand-borate glass (QSBoBa) doped with different concentrations of Nd³⁺ ions. The graph displays several absorption bands across the UV-Vis-NIR region, specifically at the wavelengths of 431, 459, 474, 515, 527, 584, 626, 683, 747, 808, and 877 nm. These bands correspond to the following energy transitions: ${}^4I_{9/2} \rightarrow {}^4D_{1/2}$, ${}^4I_{9/2} \rightarrow {}^4G_{11/2}$, ${}^4I_{9/2} \rightarrow {}^2G_{9/2}$, ${}^4I_{9/2} \rightarrow {}^4G_{7/2}$, ${}^4I_{9/2} \rightarrow {}^4G_{5/2}$, ${}^4I_{9/2} \rightarrow {}^2H_{11/2}$, ${}^4I_{9/2} \rightarrow {}^4F_{9/2}$,

Table 2. FTIR assignments of Nd3+ doped QSBoBa glasses.

Wavenumber (cm ⁻¹)	Assignments
1200 to 1400	Corresponds to the B–O asymmetric stretching vibrations in trigonal BO ₃ units.
900 to 1100	Corresponds to B-O asymmetric stretching vibrations in tetrahedral BO ₄ units.
700 to 900	Reflects B-O-B bending vibrations and contributions from other bridging oxygen linkages.

 $^4I_{9/2} \rightarrow ^4F_{7/2}, \, ^4I_{9/2} \rightarrow ^4F_{5/2}, \, ^4I_{9/2} \rightarrow ^4F_{3/2},$ respectively [4,12]. The absorption bands observed in the spectra correspond to electronic transitions within the 4f orbital of Nd³⁺ ions, which are known to be sharp and well-defined. These bands arise from transitions from the ground state ⁴I_{9/2} to various excited states. As the concentration of Nd³⁺ ions increases from 0.5 mol% to 2.0 mol%, the intensity of absorption bands increases significantly. This reflects the greater number of Nd³⁺ ions present in the glass matrix, which absorb more light at specific wavelengths corresponding to the characteristic transitions [39]. This is consistent with Beer-Lambert's law, which states that absorption is proportional to the concentration of the absorbing species (Nd3+ ions in this case). The hypersensitive nature was found at ${}^4I_{9/2} \rightarrow {}^4G_{5/2}$ transition corresponding with 584 nm shows that its intensity is highly influenced by the local symmetry and covalency of the Nd³⁺ ion environment. In more asymmetric environments, the absorption intensity tends to increase (Judd & Ofelt, 1962) [40]. The ${}^{4}\text{I}_{9/2} \rightarrow {}^{4}\text{G}_{5/2}$ transition showed a clear absorption peak, which becomes stronger as the Nd³⁺ concentration increases. The gradual increase in peak intensity with increasing Nd3+ concentration suggests a reduction in local symmetry and the introduction of more distorted ligand environments around Nd³⁺ ions [41]. This distortion likely arises from the network-modifying role of Nd3+ ions, which disrupt the borate glass structure.

Follow-up of the absorption spectrum analysis includes the oscillator strength, both experimental (f_{exp}) and calculated (f_{cal}) —for various electronic transitions of Nd3+ ions within a quartz sand-borate glass matrix, as shown in Table 3. Oscillator strength measures the probability of absorption or emission for a particular electronic transition, providing critical insights into the optical behavior of the doped glass system. The table reveals that both experimental and calculated oscillator strengths show relatively close agreement for most transitions, although some discrepancies exist for specific transitions and concentrations. As the concentration of Nd³⁺ increases, the oscillator strength values generally decrease for most transitions. The ⁴I_{9/2}→⁴G_{5/2} transition shows a decrease in f_{exp} from 18.653 for 0.5 mol% to 16.063 for 2.0 mol%. The transition ${}^{4}I_{9/2} \rightarrow {}^{2}G_{9/2}$ shows a consistent increase in intensity across concentrations. The increase in oscillator strength with higher Nd³⁺ concentrations suggests that more ions participate in the absorption processes, leading to enhanced optical absorption. This trend is consistent with the findings of Jha et al. (2012) [42] and B. Gurav et al. (2023) [43], who observed that rare-earth doped glasses show increased oscillator strengths with higher doping concentrations due to greater ion availability and interactions with the glass network. In certain transitions, the oscillator strength does not increase linearly with concentration. For example, the ⁴I_{9/2}→⁴G_{7/2} transition shows minimal increase beyond 1.5 mol%. This behavior could be related to concentration quenching effects, where close proximity between Nd3+ ions leads to non-radiative energy transfer, reduced the effective absorption strength [44]. The close match between f_{exp} and f_{cal} for many transitions suggests that the theoretical models used to calculate the oscillator strengths are valid. The RMS deviations across different doping levels are reasonably low, indicating good agreement between experimental and theoretical data. Some transitions, such as ${}^{4}I_{9/2} \rightarrow {}^{2}H_{11/2}$ and ${}^{4}I_{9/2} \rightarrow {}^{4}F_{5/2}$ show larger differences between experimental and calculated oscillator strengths. These discrepancies could result from matrix effects. Slight variations in the local environment of Nd3+ ions within the amorphous glass matrix may alter transition probabilities. Besides that, the non-radiative energy losses which are higher concentrations of Nd3+ ions can introduce non-radiative pathways, reducing experimental oscillator strengths. These discrepancies are in line with the findings of previous works, who reported that rare-earth ions in glass matrices can exhibit deviations from theoretical predictions due to subtle changes in local bonding environments [45-47].

Judd-Ofelt (JO) intensity parameters (Ω_2 , Ω_4 , Ω_6) and the spectroscopic quality factor (χ) for Nd³⁺-doped quartz sand-borate glass (QSBoBaNd) with different Nd3+ ion concentrations were shown in Table 4. The Judd-Ofelt theory provides valuable insights into the strength of optical transitions, local symmetry and the environment surrounding the rare-earth ions in glass matrices. The theory introduces three intensity parameters Ω_2 reflects the asymmetry of the local ligand field and is highly sensitive to the environment surrounding Nd³⁺ ions, Ω_4 and Ω_6 relate to the covalency of the ion-ligand bond and rigidity of the glass network [48]. Higher values of these parameters generally indicate stronger optical absorption, higher radiative transition probabilities, and enhanced luminescence efficiency. The ratio $\gamma = \Omega_4/\Omega_6$ is often used as a spectroscopic quality factor, which is a measure of the suitability of the material for laser applications. Based on the Table 6 is observed that the order of parameters is consistently Ω_6 $\Omega_2 > \Omega_4$ for all concentrations. As the known that Ω_6 has the highest value, reflecting the strength of higher multipole interactions and

Table 3. The experimental and calculation oscillator strength of Nd³⁺ doped quartz sand-Borate glass system.

Transitions λ		Eexp	QS(0.5)BoBaNd		QS(1.0)BoBaNd		QS(1.5)BoBaNd		QS(2.0)BoBaNd	
	[nm]		$f_{\rm exp}$	fcal	$f_{\rm exp}$	f cal	$f_{\rm exp}$	$f_{\rm cal}$	$f_{\rm exp}$	$f_{\rm cal}$
$^{4}I_{9/2} \rightarrow ^{4}D_{1/2}$	431	23202	0.839	0.047	0.613	0.049	0.658	0.215	0.603	0.201
${}^{4}I_{9/2} \rightarrow {}^{4}G_{11/2}$	459	21786	1.239	0.256	0.805	0.243	0.712	0.206	0.425	0.268
${}^{4}I_{9/2} \rightarrow {}^{2}G_{9/2}$	474	21097	1.269	0.458	0.963	0.438	0.977	0.391	1.119	0.498
${}^{4}I_{9/2} \rightarrow {}^{4}G_{9/2}$	515	19417	2.137	1.286	2.001	1.234	1.463	1.162	0.859	1.447
${}^{4}I_{9/2} \rightarrow {}^{4}G_{7/2}$	527	18975	3.225	2.836	2.539	2.746	3.197	2.579	3.532	3.076
${}^{4}I_{9/2} \rightarrow {}^{4}G_{5/2}$	584	17123	18.653	18.677	18.263	18.254	13.608	13.643	16.063	16.084
${}^{4}I_{9/2} \rightarrow {}^{2}H_{11/2}$	626	15974	0.045	0.240	0.022	0.229	0.074	0.180	0.097	0.241
${}^{4}I_{9/2} \rightarrow {}^{4}F_{9/2}$	683	14641	0.300	0.890	0.223	0.849	0.600	0.662	0.645	0.887
${}^{4}I_{9/2} \rightarrow {}^{4}F_{7/2}$	747	13387	6.292	4.476	5.454	4.265	4.487	3.199	5.881	4.361
${}^{4}I_{9/2} \rightarrow {}^{4}F_{5/2}$	808	12376	5.988	7.156	6.104	6.833	4.865	5.728	6.556	7.495
${}^{4}I_{9/2} \rightarrow {}^{4}F_{3/2}$	877	11403	1.780	1.032	1.584	0.996	1.784	1.294	2.245	1.483
$\delta_{\rm rms}$				0.891		0.623		0.598		0.673

Table 4. Judd-Ofelt intensity parameters (x 10^{-20}) and spectroscopic quality factor χ (Ω_4/Ω_6) of QSBoBaNd glasses and other reported Nd³⁺ glasses.

Glass samples	Ω_2	Ω_4	Ω_6	$\chi\left(\Omega_4/\Omega_6 ight)$	Trend
QS(0.5)BoBaNd	7.5189	0.3627	9.4292	0.038	$\Omega_6 > \Omega_2 > \Omega_4$
QS(1.0)BoBaNd	6.9485	0.3584	8.4971	0.042	$\Omega_6 > \Omega_2 > \Omega_4$
QS(1.5)BoBaNd	4.5212	1.5585	6.2595	0.249	$\Omega_6 > \Omega_2 > \Omega_4$
QS(2.0)BoBaNd	5.4191	1.4489	8.4804	0.171	$\Omega_6 \! > \Omega_2 \! > \Omega_4$
NBS0.5 [29]	5.74	1.73	7.18	0.24	$\Omega_6 \! > \Omega_2 \! > \Omega_4$
BSKNLNd10 [58]	9.93	8.05	8.35	0.97	$\Omega_2 > \Omega_6 > \Omega_4$
NaLiCdBNd05 [59]	3.35	4.99	3.89	1.28	$\Omega_4 > \Omega_6 > \Omega_2$

Table 5. Emission peak wavelength (λp), effective bandwidth ($\Delta \lambda_{eff}$), emission cross-section ($\sigma_e \times 10^{-20}$), branching ratio (β), radiative transition probability (ΔR) and radiative lifetime of Nd³⁺ doped QSBoBa glasses.

Glass samples	Transitions	λ_{p}	$\Delta \lambda_{ m eff}$	$\sigma_{e}(\lambda_{p})$	β_{exp}	β_{cal}	$\mathbf{A}_{\mathbf{R}}$		$ au_{ m R}$
	$^4\mathrm{F}_{3/2}$ \longrightarrow				[%]	[%]	[s ⁻¹]	J-O	Exp
		[nm]	[nm]	[cm ²]				[µs]	[µs]
	$^{4}I_{9/2}$	913	36.70	0.58	0.02	0.18	552.53		
QS(0.5)BoBaNd	$^{4}I_{11/2}$	1060	37.94	3.75	0.70	0.65	2035.41	319	102
	$^{4}I_{13/2}$	1330	52.11	1.73	0.30	0.17	520.16		
	$^{4}I_{9/2}$	913	26.42	0.77	0.02	0.18	581.97		
QS(1.0)BoBaNd	$^{4}I_{11/2}$	1060	37.87	3.56	0.69	0.65	2117.79	306	81
	$^{4}I_{13/2}$	1330	53.50	1.59	0.31	0.17	539.94		
	⁴ I _{9/2}	913	33.03	0.80	0.02	0.26	767.04		
QS(1.5)BoBaNd	$^{4}I_{11/2}$	1060	40.62	2.67	0.71	0.59	1747.60	338	71
	$^{4}I_{13/2}$	1330	53.65	1.20	0.29	0.14	416.32		
	$^{4}I_{9/2}$	913	37.22	0.81	0.03	0.23	891.29		
QS(2.0)BoBaNd	$^{4}I_{11/2}$	1060	39.95	3.62	0.69	0.61	2348.69	260	55
	$^{4}I_{13/2}$	1330	58.28	1.50	0.31	0.14	573.96		

the rigidity of the glass network. Moreover, Ω_2 , associated with the asymmetry of the Nd3+ environment, decreases with increasing Nd3+ concentration [49]. The decreasing Ω_2 parameter suggests that the local asymmetry around Nd3+ ions reduces as the concentration of Nd3+ increases. This may indicate that at higher concentrations, the Nd³⁺ ions experience a more symmetric environment within the glass network, potentially due to clustering or saturation effects [50]. The $\Omega_6 > \Omega_2 > \Omega_4$ trend indicates that the rigidity of the glass matrix dominates the optical properties of the doped glass. Such a trend is consistent with borate-based glasses, where the network structure remains robust even with the incorporation of rare-earth ions [51]. A higher quality factor (χ) indicates better suitability for laser applications. The value of χ high when Nd³⁺ concentration is more than 1 mol% suggests that the glass becomes increasingly efficient in supporting radiative transitions, making it more appropriate for use in laser materials [44]. This trend aligns with the fact that an optimal balance between rigidity (Ω_6) and covalency (Ω_4) is necessary for enhanced luminescence and laser performance. Figure 6 illustrates the photoluminescence (PL) spectra of Nd³⁺-doped quartz sand-borate glass (QSBoBa) for various concentrations of Nd³⁺ ions (0.5, 1.0, 1.5, and 2.0 mol%).

3.5 Photoluminescence spectra

The photoluminescence spectra provide critical insights into the luminescence behavior, emission transitions, and energy transfer dynamics within the glass matrix. The emission peaks observed in the spectra correspond to transitions from the excited state 4F3/2 to various lower energy states $^4I_{9/2}$, $^4I_{11/2}$, and $^4I_{13/2}$ with corresponding to the 913 nm, 1060 nm, and 1330 nm wavelength respectively. These

emissions are characteristic of Nd3+ ions, which undergo intra 4f electronic transitions that are largely shielded from the surrounding environment by the 5s and 5p orbitals, resulting in sharp, well-defined emission peaks [52]. The ${}^{4}F_{3/2} \rightarrow {}^{4}I_{11/2}$ transition with 1060 nm wavelength been dominant peak in the spectrum, commonly observed in Nd³⁺-doped materials. This transition lies in the near-infrared (NIR) region and is crucial for laser applications, especially in solid-state lasers such as Nd. From the Figure 6 also observed the effect of Nd³⁺ concentration on the emission intensity. The emission intensity slightly decreased as the Nd3+ ion concentration increased from 0.5 mol% to 1.0 mol%. The decrease in intensity at higher concentrations suggests the onset of concentration quenching, a common phenomenon in rareearth doped materials. In concentration quenching, non-radiative energy transfer occurs between closely spaced Nd³⁺ ions, resulting in energy losses via non-radiative decay pathways [53]. In Nd³⁺-doped glasses, cross-relaxation and energy migration between neighboring Nd³⁺ ions can lead to concentration quenching. When Nd³⁺ ions are in close proximity (as seen at higher doping levels), excited-state energy is transferred between ions, increasing the probability of non-radiative decay. This results in reduced luminescence intensity. Based on the observed spectra, the 0.5 mol% Nd³⁺ concentration offers the highest emission intensity without significant quenching. This makes it an ideal doping concentration for applications requiring high luminescence efficiency, such as optical amplifiers and solid-state lasers.

The further observations for optical properties of Nd^{3+} doped QSBoBa glass system is shown in Table 5. From the table is known that the effective bandwidth ($\Delta\lambda_{eff}$) increases with Nd^{3+} concentration, especially for the 1330 nm transition, reaching 58.28 nm at 2.0 mol%. Broadening of the bandwidth with increasing Nd^{3+} concentration

suggests enhanced structural disorder in the glass matrix, a common effect in rare-earth doped glasses [54]. This broadening can improve the glass's performance in broadband optical amplifiers. The emission at 1060 nm is particularly significant, as it matches the wavelength of Nd lasers, making the material suitable for laser gain media. Moreover, the emission cross-section (σ_e) increases with Nd³⁺ concentration for all transitions, with the 1060 nm transition showing the highest values. At 0.5 mol%, σ_e reaches 3.75×10^{-20} cm². A higher emission cross-section indicates stronger radiative emissions and greater efficiency in light amplification [55]. Whereas the experimental branching ratio (β_{exp}) for the 1060 nm transition remains around 0.69 across all concentrations, indicating that this transition dominates radiative emissions from the ⁴F_{11/2} level. A high branching ratio for the 1060 nm transition indicates that a significant fraction of the excited-state population decays radiatively to the ⁴I_{11/2} state, which is crucial for achieving high laser gain [56]. This makes the material particularly suited for Nd-based laser devices

Figure 7 presents the normalized intensity *vs.* time decay curves for the photoluminescence lifetime measurements of Nd³⁺-doped quartz sand-borate (QSBoBa) glass system. The figure found that the decay curves follow an exponential trend typical of Nd³⁺ ion-doped systems, reflecting the natural decay of excited-state populations. The measured decay time values were 120 μs, 81 μs, 71 μs, and 55 μs, corresponding to QS(0.5)BoBaNd, QS(1.0)BoBaNd, QS(1.5)BoBaNd and QS(2.0) BoBaNd, respectively. The decay became steeper with increasing Nd³⁺ concentration, indicating a reduction in the effective photoluminescence lifetime. The curves for 0.5 mol%, and 1.0 mol% showed slower decay rates, suggesting longer lifetimes than the higher concentrations (1.5 mol%, and 2.0 mol%).

In the Table 6 also presented highlights the radiative properties for the ${}^4F_{3/2} \rightarrow {}^4I_{11/2}$ transition of Nd³⁺-doped quartz sand-borate glass (QSBoBa) with varying Nd³⁺ ion concentrations (0.5, 1.0, 1.5, and 2.0 mol%). The radiative transition probability (AR) increases from 2035.41 s^{-1} (0.5 mol%) to 2348.69 s^{-1} (2.0 mol%). When compared with other systems, QSBoBa glass shows higher radiative probabilities than BSNNd0.5 [48] but slightly lower than BSKNLNd05 [60] and NaLiCdBNd05 glasses [59]. Higher AR values indicate a greater probability of radiative transitions, which is essential for achieving high laser gain medium. QSBoBa glasses, with their increasing AR values, demonstrate good potential for solid-state laser applications. The steady increase in AR with Nd3+ concentration suggests that the Nd³⁺ ions are effectively incorporated into the glass network, enhancing their emission properties. The reduction in lifetime with increasing Nd³⁺ concentration is attributed to concentration quenching, where non-radiative energy transfer processes between Nd3+ ions increase as their spatial proximity becomes closer [60,61]. At higher concentrations (1.5 mol% and 2.0 mol%), ion-ion interactions dominated, leading to cross-relaxation and energy migration, which accelerate the decay rate and shorten the measured lifetime [59]. Non-radiative energy transfer occurs between closely spaced Nd³+ ions, which leads to energy losses through heat dissipation instead of light emission. This effect becomes more significant as the ion concentration increases, explaining the shorter lifetimes observed at 1.5 mol% and 2.0 mol% [62]. Cross-relaxation processes, where one excited Nd³+ ion transfers energy to a neighboring ion in the ground state, further reduce the effective lifetime. The 0.5 mol% and 1.0 mol% samples show the most stable decay profiles with longer lifetimes, indicating minimal quenching effects. These concentrations are likely close to the optimal doping range for maximizing emission efficiency without significant losses from non-radiative processes [63].

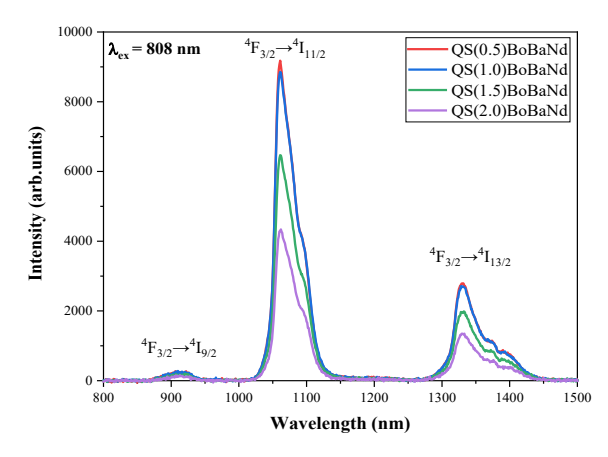


Figure 6. Emission spectra of Nd³⁺ doped quartz sand-borate glass system with Nd³⁺ ion concentration of 0, 0.5, 1.0, 1.5, and 2.0 mol%.

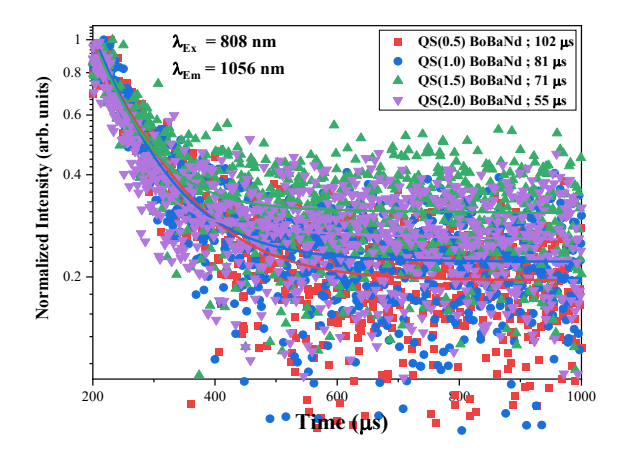


Figure 7. The exponential lifetime of the quartz sand BoBaNd glass with the Nd³⁺ ion concentration is 0; 0.5; 1.0; 1.5; and 2.0 mol%.

Table 6. Radiative properties special for ${}^4F_{3/2} \rightarrow {}^4I_{11/2}$ of the Nd³⁺ doped quartz sand-Borate glass system with the Nd³⁺ ion concentration is 0, 0.5, 1.0, 1.5, and 2.0 mol% and compared with the others samples.

Glass samples	A _R [s ⁻¹]	$\sigma_{\rm e} (\lambda_{\rm p}) [{\rm cm}^2]$	η [%]	Ref.
QS(0.5)BoBaNd	2035.41	3.75	31.97	Present
QS(1.0)BoBaNd	2117.79	3.56	26.47	Present
QS(1.5)BoBaNd	1747.60	2.67	21.01	Present
QS(2.0)BoBaNd	2348.69	3.62	21.15	Present
BSNNd0.5	1760.50	0.24	22.98	Madhu et al., 2023 [57]
BSKNLNd10	2665	5.84	87	Deepa et al., 2019 [58]
NaLiCdBNd05	2932	5.69	86	Deepa et al., 2021 [59]

4. Conclusion

This study was analyzed the structural, spectroscopic and radiative properties of the Nd³⁺-doped quartz sand-borate glass (QSBoBa) system with Nd³⁺ ion concentrations of 0, 0.5, 1.0, 1.5 and 2.0 mol%. The introduction of Nd₂O₃ (Neodymium Oxide) was aimed at tuning the optical and radiative properties of the glasses. The increasing Nd³⁺ ion concentration had acted as a network modifier, disrupted the borate structure and introduced non-bridging oxygen (NBO) atoms, which had contributed to the observed structural and optical changes. The optical absorption spectra revealed several prominent absorption bands, particularly the ${}^{4}\text{I}_{9/2} \rightarrow {}^{4}\text{G}_{5/2}$ hypersensitive transition around 584 nm. The photoluminescence emission spectra showed strong transitions from the excited state ⁴F_{3/2} to several lower energy states including the ⁴I_{9/2}; ⁴I_{11/2} and ⁴I_{13/2} levels. The 1060 nm transition was the most intense and significant for laser applications. The exponential decay lifetimes of the photoluminescence signal confirmed the concentration quenching effect. The lifetimes for the 0.5 mol% and 1.0 mol% samples were longer, reflecting efficient radiative decay. However, as the concentration increased to 1.5 mol% and 2.0 mol%, the lifetime shortened significantly due to enhanced ion-ion interactions, which promoted non-radiative energy transfer processes such as cross-relaxation and energy migration between neighboring Nd³⁺ ions.

Acknowledgement

This project was made possible thanks to financial support from the Ministry of Education, Culture, Research and Technology (MoECRT) Republic of Indonesia (grant number 068/E5/PG.02.00.PL/2024) and Universitas Negeri Medan for the research collaboration scheme. We are also grateful to Thailand Science Research and Innovation (TSRI) and Nakhon Pathom Rajabhat University for supporting this research. This research has received funding support from the NSRF via the Program Management Unit for Human Resources & Institutional Development, Research and Innovation [grant number B41G670028]. This research was partially supported by Chiang Mai University.

References

- [1] M. Kumar, M. K. Sahu, S. Kaur, A. Prasad, R. Bajaj, R. A, Talewar, Y. Tayal, K. Swapna, and A. S. Rao, "Visible and NIR spectral analysis of Er³⁺ doped LiBiAlBSi glasses for laser applications," *Journal of Materials Science: Materials in Electronics*, vol. 35, no. 7, p. 504, 2024.
- [2] V. B. Sreedhar, N. Vijaya, D. Ramachari, and C. K. Jayasankar, "Luminescence studies on Er³⁺-doped zincfluorophosphate glasses for 1.53 µm laser applications," *Journal of Molecular Structure*, vol. 1130, pp. 1001-1008, 2017.
- [3] H. M. Elsaghier, M. A. Azooz, N. A. Zidan, W. Abbas, A. Okasha, and S. Y. Marzouk, "Spectroscopic and optical investigations on Er³⁺ ions doped alkali cadmium phosphate glasses for laser applications," *Journal of Non-Crystalline Solids*, vol. 588, p. 121616, 2022.
- [4] A. S. Alves, N. S. Camilo, C. S. José Filho, J. E. Mabjaia, V. Pilla, N. O. Dantas, and A. A., Andrade, "Photoluminescence-

- based temperature sensing in Nd³⁺-Doped tellurite glasses," *Journal of Luminescence*, vol. 280, p.121090, 2025.
- [5] M. M. Ismail, I. K. Batisha, L. Zur, A. Chiasera, M. Ferrari, and A. Lukowiak, "Optical properties of Nd³⁺-doped phosphate glasses," *Optical Materials*, vol. 99, p. 109591, 2020.
- [6] M. Shoaib, G. Rooh, N. Chanthima, H. J. Kim, and J. Kaewkhao, "Luminescence properties of Nd³⁺ ions doped P₂O₅-Li₂O₃-GdF₃ glasses for laser applications," *Optik*, 199, p. 163218, 2019.
- [7] J. Rajagukguk, M. Djamal, R. Hidayat, S. Suprijadi, A. Amminudin, Y. Ruangtaweep, and J. Kaewkhao, "Optical properties of Nd³⁺ doped phosphate glasses at ⁴F₃₂→ ⁴I_{11/2} hypersensitive transitions," *The journal of pure and applied chemistry research*, vol. 5, no. 3, p.148, 2016.
- [8] A. Kheloufi, E. Bobocioiu, F. Kerkar, A. Kefaifi, S. Anas, S. A. Medjahed, Y. Belkacem, and A. Keffous, "Optical and spectroscopic characterizations of algerian silica raw material to predict high quality solar-grade silicon," *Optical Materials*, vol. 65, pp. 142-149, 2017.
- [9] J. Bhemarajam, P. S. Prasad, M. M. Babu, and M. Prasad, "Spectroscopic and optical investigations on Er³⁺/Yb³⁺ co-doped bismuth–boroleadlithium glasses for solid state laser applications," *Optical Materials*, vol. 122, p. 111657, 2021.
- [10] J. Rajagukguk, R. Situmorang, M. Djamal, R. Rajaramakrishna, J. Kaewkhao, and P. H. Minh, "Structural, spectroscopic and optical gain of Nd³⁺ doped fluorophosphate glasses for solid state laser application," *Journal of Luminescence*, vol. 216, p. 116738, 2019.
- [11] A. Jose, T. Krishnapriya, J. R. Jose, C. Joseph, and P. R. Biju, "NIR photoluminescent characteristics of Nd³⁺ activated fluoroborosilicate glasses for laser material applications," *Physica B: Condensed Matter*, vol. 634, p. 413772, 2022.
- [12] G. Lakshminarayana, K. M. Kaky, S. O. Baki, A. Lira, A. N. Meza-Rocha, C. Falcony, U. Caldiño, I. V. Kityk, A. Méndez-Blas, A. F. Abas, and M. T. Alresheedi, "Nd³+-doped heavy metal oxide based multicomponent borate glasses for 1.06 μm solid-state NIR laser and O-band optical amplification applications," *Optical Materials*, vol. 78, pp. 142-159. 2018.
- [13] S. Kang, X. Wang, W. Xu, X. Wang, D. He, and L. Hu, Effect of B₂O₃ content on structure and spectroscopic properties of neodymium-doped calcium aluminate glasses," *Optical Materials*, vol. 66, pp. 287-292, 2017.
- [14] J. Rajagukguk, R. Hidayat, S. Suprijadi, M. Djamal, Y. Ruangtaweep, M. Horprathum, and J. Kaewkhao, Structural and optical properties of Nd³⁺ doped Na₂O-PbO-ZnO-Li₂O-B₂O₃ glasses system," *Key Engineering Materials*, vol. 675, pp. 424-429, 2016.
- [15] M. M., Ismail, Y. M. Hamdy, and H. A. Abo-Mosallam, Enhancing of ⁴F_{3/2}→ ⁴I_{9/2} transition of Nd³⁺ doped BaO-Ga₂O₃−Al₂O₃− B₂O₃ glasses for near-infrared laser applications," *Journal of Luminescence*, vol. 263, p. 120014, 2023.
- [16] J. Abellan-garcia, D. M. Martinez, M. I. Khan, Y. M. Abbas, F. Pellicer-marti, and F. Pellicer-Martínez, "Environmentally friendly use of rice husk ash and recycled glass waste to produce ultra-high-performance concrete," *Journal of Materials Research* and Technology, vol. 25, pp. 1869–1881, 2023.

- [17] S. K. S. Hossain, L. Mathur, P. K. Roy, S. K. S. Hossain, L. Mathur, and P. K. R. Rice, "Rice husk/rice husk ash as an alternative source of silica in ceramics: A review," *Journal of Asian Ceramic Societies*, vol. 6, pp. 299–313, 2018.
- [18] J. Rajagukguk, D. H. Rajagukguk, R. A. Syahputra, H. Fibriasari, C. S. Sarumaha, K. Kirdsiri, S. Kothan, and J. Kaewkhao, "Radioluminescence properties of huta ginjang quartz sand doped with CeF₃ and Tb₂O₃ for scintillator application," Radiation Physics and Chemistry, vol. 223, p. 111939, 2024.
- [19] S. Ravangvong, S. Khunnarong, S. Temmawat, S. Chaichalerm, W. Nissapa, K. Pinnak, B. Sriumnuay, K. Sriwongsa, P. Glumglomchit, P. Boonsang, Y. Ruangtaweep, and J. Kaewkhao, "Glass production from rice husk ash as an imitation gemstone products," *Materials Today: Proceedings*, vol. 65, pp. 2376– 2379, 2022.
- [20] Y. Ruangtaweep, J. Kaewkhao, C. Kedkaew, and P. Limsuwan, "Investigation of biomass fly ash in Thailand for recycle to glass production," *Procedia Engineering*, vol. 8, pp. 58–61, 2011.
- [21] N. A. Soliman, and A. Tagnit-Hamou, "Using glass sand as an alternative for quartz sand in UHPC," *Construction and Building Materials*, vol. 145, pp. 243–252, 2017.
- [22] N. Srisittipokakun, N. Singkiburin, and J. Kaewkhao, "Study properties of Cr₂O₃ doped in glasses prepared from sugar cane ash," *Thai Interdisciplinary and Sustainability Review*, vol. 14, pp. 16–19, 2019.
- [23] S. A. Umar, M. K. Halimah, K. T. Chan, and A. A. Latif, "Physical, structural and optical properties of erbium doped rice husk silicate borotellurite (Er-doped RHSBT) glasses," *Journal of Non-Crystalline Solids: X*, vol. 472, pp. 31–38, 2017.
- [24] X. Wang, H. Liu, Z. Wang, Y. Ma, and G. M. Kale, "Effect of rare earth oxides on the properties of bio-soluble alkaline earth silicate fibers," *Journal of Rare Earths*, vol. 34, pp. 203–207. 2016.
- [25] Z. T. Ye, Y. M. Pai, C. H. Lin, L. C. Chen, H. T. Nguyen, and H. C. Wang, "Nanoparticle-doped polydimethylsiloxane fluid enhances the optical performance of AlGaN-based deep-ultraviolet light-emitting diodes," *Nanoscale Research Letters*, vol. 14, 2019.
- [26] J. Rajagukguk, P. Simamora, L. Sitinjak, E. Simanullang, C. S. Sarumaha, N. Intachai, S. Kothan, and J. kaewkhao, "NIR luminescence properties of Nd³⁺ ion doped glasses medium based on Huta Ginjang quartz sand," *Radiation Physics and Chemistry*, vol. 229, p. 112466, 2025.
- [27] J. Rajagukguk, J. H. Panggabean, C. S. Sarumaha, P. Kanjanaboos, N. Phuphathanaphong, S. Kothan, J. Kaewkhao, and M. Djamal, Luminescence properties and energy transfer of Nd³⁺-Er³⁺/ Nd³⁺-Pr³⁺ co-doped LFP glasses system," *Heliyon*, vol. 9, no. 11, 2023.
- [28] W. J. Faria, T. D. S. Gonçalves, and A. S. de Camargo, "Near infrared optical thermometry in fluorophosphate glasses doped with Nd³⁺ and Nd³⁺/Yb³⁺," *Journal of Alloys and Compounds*, vol. 883, p.160849, 2021.
- [29] Y. Tayal, R. A. Talewar, S. Mahamuda, K. Maheshwari, S. Kumari, M. Kumar, R. Pilania, A. Prasad, and A. S. Rao, "Enhanced emission in the NIR range by Nd³⁺ doped borosilicate

- glass for lasing applications," *Applied Physics B*, vol. 130, no. 9, p. 157, 2024.
- [30] N. S. Ezra, I. S. Mustafa, M. I. Sayyed, K. K. Dakok, I. M. Fadhirul, T. H. Khazaalah, G. I. Efenji, M. Jamil, H. S. Naeem, A. O. Oke, and A. S. A. Idriss, "Synthesis, and impact of GaN deposition on the physical, optical, and structural properties of Nd³⁺-doped Na₂O borate glasses prepared with soda lime (SLS) glass as a silica source," *Optical Materials*, vol. 155, p. 115907, 2024.
- [31] J. Rajagukguk, D. H. Rajagukguk, R. S. Gultom, P. Simamora, R. Situmorang, and C. Sarumaha, "Structure and emission properties of Nd³⁺ doped oxyfluorophosphate glasses," *Journal* of *Physics: Conference Series*, vol. 2193, no. 1, p. 012007, 2022.
- [32] A. Marzuki, R. W. Astuti, D. E. Fausta, F. I. Kasy, and M. A. Mahasindi, "Impact of Nd₂O₃ on physical properties of lead borate glass system," *Journal of Physics: Theories and Applications*, vol. 7, no. 2, pp. 115-123, 2023.
- [33] I. Kashif, A. Abd El-Maboud, and A. Ratep, "Effect of Nd₂O₃ addition on structure and characterization of lead bismuth borate glass," *Results in Physics*, vol. 4, pp. 1-5, 2014.
- [34] S. Biradar, A. Dinkar, A. S. Bennal, G. B. Devidas, B. T. Hareesh, M. K. Siri, K. N. Nandan, M. I. Sayyed, H. Es-soufi, and M. N. Chandrashekara, Comprehensive investigation of borate-based glasses doped with BaO: An assessment of physical, structural, thermal, optical, and radiation shielding properties," *Optical Materials*, vol. 150, p. 115176, 2024.
- [35] D. Sidebottom, R. Bergman, L. Börjesson, and L. M. Torell, "Two-step relaxation decay in a strong glass former," *Physical review letters*, vol. 71, no. 14, p. 2260, 1993.
- [36] H. A. Abo-Mosallam, M. A. Azooz, and E. A. Mahdy, "Enhancement the crystallization and electro-magnetic properties of BaO–Al₂O₃–B₂O₃ glass ceramics doped with Nd₂O₃-rare earth," *Scientific Reports*, vol. 13, no. 1, p. 18262. 2023.
- [37] S. F. Hathot, B. M. Al Dabbagh, and H. Aboud, "Structural and spectroscopic correlation in barium-boro-tellurite glass hosts: effects of Dy₂O₃ doping," *Chalcogenide Letters*, vol. 21, no. 2, 2024.
- [38] F. A. Abdel-Wahab, A. M. Fayad, M. Abdel-Baki, and H. AbdelMaksoud, "Role of non-bridging oxygen defect in the ionic conductivity and associated oxygen trap centers in lead-borate oxide glass: Effect of structural substitution of PbO for Ag2O and Li2O modifiers," *Journal of Non-Crystalline Solids*, vol. 500, pp.84-91, 2018.
- [39] A. Madhu, S. A. Idris, N. S. Abd El-Gawaad, V. B. Tangod, and N. Srinatha, "Structural, elastic and optical properties of rare earth ions (Nd³⁺, Dy³⁺ & Nd³⁺/Dy³⁺) incorporated B₂O₃+ K₂O + ZnO + ZnF₂ glasses, "Journal of Molecular Structure, vol. 1294, p. 136445, 2023.
- [40] P. R. Rani, M. Venkateswarlu, K. Swapna, S. Mahamuda, R. A. Talewar, C. B. A. Devi, and A. S. Rao, "NIR photoluminescence studies of Nd³⁺ doped B₂O₃–BaF₂–PbF₂–Al₂O₃ glasses for 1.063 μm laser applications," *Journal of luminescence*, vol. 229, p. 117701, 2021.
- [41] Y. Zhang, Z. Zhou, W. Li, Y. Yang, B. Mei, and Z. Sun, "The effect of Nd³⁺ concentration on fabrication, microstructure,

- and luminescent properties of anisotropic S-FAP ceramics," *Journal of the American Ceramic Society*, vol. 105, no. 4, pp. 2932-2944, 2022.
- [42] A. Jha, B. Richards, G. Jose, T. Teddy-Fernandez, P. Joshi, X. Jiang, and J. Lousteau, "Rare-earth ion doped TeO₂ and GeO₂ glasses as laser materials," *Progress in Materials Science*, vol. 57, no. 8, pp. 1426-1491, 2012.
- [43] B. Gurav, G. B. Devidas, A. Dinkar, and S. Biradar, "Neodymium doped borate glasses for nir emitting solid state device applications," *Indian Journal of Science and Technology*, vol. 16, no.06, pp. 435-441, 2023.
- [44] S. Khan, S. K. Mohapatra, S. Chakraborty, and K. Annapurna, "Energy transfer mechanisms and non-radiative losses in Nd³⁺ doped phosphate laser glass: Dopant concentration effect study," *Optical Materials*, vol. 143, p. 114229, 2023.
- [45] B. Charfi, M. Zekri, A. Herrmann, K. Damak, and R. Maâlej, "Atomic scale network structure of a barium aluminosilicate glass doped with different concentrations of rare-earth ions explored by molecular dynamics simulations," *Computational Materials Science*, vol. 218, p. 111965, 2023.
- [46] C. Calahoo, and L. Wondraczek, "Ionic glasses: Structure, properties and classification," *Journal of Non-Crystalline Solids:* X, vol. 8, p. 100054, 2020.
- [47] N. Boudchicha, M. Iezid, F. Goumeidane, M. Legouera, P. S. Prasad, and P. V. Rao, "Judd-Ofelt analysis and spectroscopy study of tellurite glasses doped with rare-earth (Nd³⁺, Sm³⁺, Dy³⁺ and Er³⁺)," *Materials*, vol. 16, no. 21, p. 6832, 2023.
- [48] L. Smentek, "Judd-Ofelt theory: Past, present and future," *Molecular Physics*, vol. 101, no. 7, pp. 893-897, 2003.
- [49] K. U. Kumar, V. A. Prathyusha, P. Babu, C. K. Jayasankar, A. S. Joshi, A. Speghini, and M. Bettinelli, Fluorescence properties of Nd³⁺-doped tellurite glasses," *Spectrochimica Acta Part A: Molecular and Biomolecular Spectroscopy*, vol. 67, no. 3-4, pp. 702-708, 2007.
- [50] S. S. Yaacob, M. R. Sahar, F. Mohd-Noor, W. W. Shamsuri, S. M. Zain, N. A. M. Jan, M. F. Omar, S. A. Jupri, S. M. Aziz, and A. S. Alqarni, "The effect of Nd₂O₃ content on the properties and structure of Nd³⁺ doped TeO₂–MgO–Na₂O-glass," *Optical Materials*, vol. 111, p. 110588, 2021.
- [51] S. B. Kolavekar, N. H. Ayachit, R. Rajaramakrishna, N. G. Pramod, and J. Kaewkhao, "Reddish-orange emission and Judd-Ofelt investigation of Sm³⁺ ions doped in zince-bismuth-phospho-tellurite glasses for solid lighting application," *Journal of Luminescence*, vol. 226, p. 117498, 2020.

- [52] W. T. K. Chan, and W. T. Wong, "Recent development in lanthanide coordination compounds for biomedical imaging applications," *Polyhedron*, vol. 83, pp. 150-158, 2014.
- [53] Y. Cao, Y. Yang, C. Huang, H. Chi, X. Li, Y. Gan, Z. Hou, and G. Zhou, "A Nd-doped silica glass with high doping concentration, low hydroxyl content, and 900 nm fluorescence emission fabricated by laser additive manufacturing," *Ceramics International*, vol. 50, no. 23, Part B, pp. 51297-51306, 2024.
- [54] V. R. Kumar, B. N. Kumar Reddy, R. G. Naga, and P. S. Prasad, "Spectroscopic properties of Nd³⁺ ions in LiO₂-MO-Sb₂O₃ glasses," *Optik*, vol. 264, 2022.
- [55] G. L. Agawane, K. Linganna, J. H. In, and J. H. Choi, "High emission cross-section Er³⁺-doped luorophosphate glasses for active device application," *Optik*, vol. 198, p. 163228, 2019.
- [56] C. Strohhöfer, P. G. Kik, and A. Polman, "Selective modification of the Er^{3+ 4}I_{11/2} branching ratio by energy transfer to Eu³⁺," *Journal of Applied Physics*, vol. 88, no. 8, pp. 4486-4490, 2000.
- [57] A. Madhu, M. Al-Dossari, N. S. Abd EL-Gawaad, D. Gelija, K. N. Ganesha, and N. Srinatha, "Structural, optical and luminescence properties of Nd³⁺ ions in B₂O₃+ SiO₂+ TeO₂+ Na₂O glasses," *Optical Materials*, vol. 136, p. 113436, 2023.
- [58] M. Deepa, R. Doddoji, C. S. D. Viswanath, and A. V. Chandrasekhar, "Optical and NIR luminescence spectral studies: Nd³⁺-doped borosilicate glasses," *Journal of Luminescence*, vol. 213, pp. 191–196, 2019.
- [59] M. Deepa, R, Doddoji, and A. V. Chandrasekhar, "NIR emission from Nd³⁺-doped Na₂O+Li₂O+CdO+B₂O₃ glasses: A study of structural, physical and radiative properties," *Journal of Optics*, vol. 50, pp. 278-288, 2021.
- [60] P. Ramprasad, C. Basavapoornima, S. R. Depuru, and C. K. Jayasankar, "Spectral investigations of Nd³⁺:Ba(PO₃)₂+La₂O₃ glasses for infrared laser gain media applications," *Optical Materials*, vol. 129, p. 112482, 2022.
- [61] K. S. Rao, V. R. Kumar, Y. Zhydachevskii, A. Suchocki, M. Piasecki, Y. Gandhi, V. R. Kumar, and N. Veeraiah, "Luminescence emission features of Nd³⁺ ions in PbO–Sb₂O₃ glasses mixed with Sc₂O₃/Y₂O₃/HfO₂," *Optical Materials*, vol. 69, pp. 181-189, 2017.
- [62] W. E. K. Gibbs, D. J. Booth, and V. K. Bogdanov, "Population dynamics of the ³F₄ and ³H₄ levels in highly-doped Tm³⁺: ZB(L)AN glasses," *Journal of non-crystalline solids*, vol. 353, no. 1, pp. 1-5, 2007.
- [63] R. Shi, and A. V. "Mudring, phonon-mediated nonradiative relaxation in Ln³⁺-doped luminescent nanocrystals," ACS Materials Letters, vol. 4, no. 10, pp. 1882-1903, 2022.